Title	Cyclic and Tangential Plasticity Effects for the Buckling Behavior of a Thin Wall Pier under Multiaxial and Non-proportional Loading Conditions
Author(s)	Momii, Hideto; Tsutsumi, Seiichiro; Fincato, Riccardo
Citation	Transactions of JWRI. 2015, 44(1), p. 41-47
Version Type	VoR
URL	https://doi.org/10.18910/57262
rights	
Note	

Cyclic and Tangential Plasticity Effects for the Buckling Behavior of a Thin Wall Pier under Multiaxial and Non-proportional Loading Conditions†

MOMII Hideto*, TSUTSUMI Seiichiro** and FINCATO Riccardo***

Abstract

We have adopted an unconventional elastoplastic model capable of taking into account the generation of the inelastic strain rate not only along the direction normal to the yield surface but also along the tangential one. In this paper the aforementioned model has been studied by applying a series of non-proportional loading paths to a thin wall pier and comparing the results obtained with the ones derived by neglecting the tangential contribution.

KEY WORDS: (non-proportional loading), (tangential plasticity), (cyclic plasticity), (buckling)

1. Introduction

Numerous experimental and numerical simulation investigations of thin wall bridge piers, evaluating seismic capacity and aseismic retrofit, have been conducted since the Hyogoken-Nanbu earthquake on 17th January 1995. Most of these works considered only uni-directional load in lateral direction of the pier. Seismic excitations, however, are naturally quite complex, the seismic excitation amplitude changes during earthquake as well as its direction, which usually is not uni-directional but rather bi-directional and non-proportional in lateral direction. Therefore, in order to correctly design the structural stiffness for those conditions, several cyclic non-proportional loadings have been investigated in this work.

In this paper an unconventional elastoplastic constitutive model based on the Extended Subloading Surface model with additional modifications to catch the so-called "Tangential Plasticity"[1]-[5] , has been adopted for the numerical analyses. This theory allows to take into account the contributions of the plastic deformations, even within the elastic domain of conventional plasticity theories, and the tangential inelastic strain induced by a stress rate component tangential to the plastic potential surface. Experimental results have been compared with the numerical ones carried out including or not the effect of tangential plasticity.

2. Tangential Plasticity Constitutive equations
2.1 Basic description of extended subloading surface model

In the present work the extended subloading surface model[2], in the form of the cutting-plane return mapping method[3][4][6], has been adopted for a fast and accurate computation.

For sake of brevity, the extended subloading surface constitutive equations and its return mapping formulation will not presented in the present paper; the reader is referred to the lecture notes[2] for a full and detailed explanation of the theory. As a general description of the model it can be mentioned here that the smooth transition from elastic and plastic domains is achieved by adding a new loading surface (i.e. subloading surface), which is created by means of a similarity transformation from the conventional yield one. The insertion of a mobile similarity center enriches further the formulation, allowing to a more realistic description of the irreversible strain accumulation during cycling loading.

2.2 Extension to the tangential plasticity

Most of the conventional plasticity models, and unconventional one as well, adopt an associate flow rule for the definition of the plastic strain rate/increment. Under this assumption it is possible to catch a realistic response in case of proportional loading paths, where the ratio

Cyclic and Tangential Plasticity Effects for the Buckling Behavior of a Thin Wall Pier under Multiaxial and Non-proportional Loading Conditions
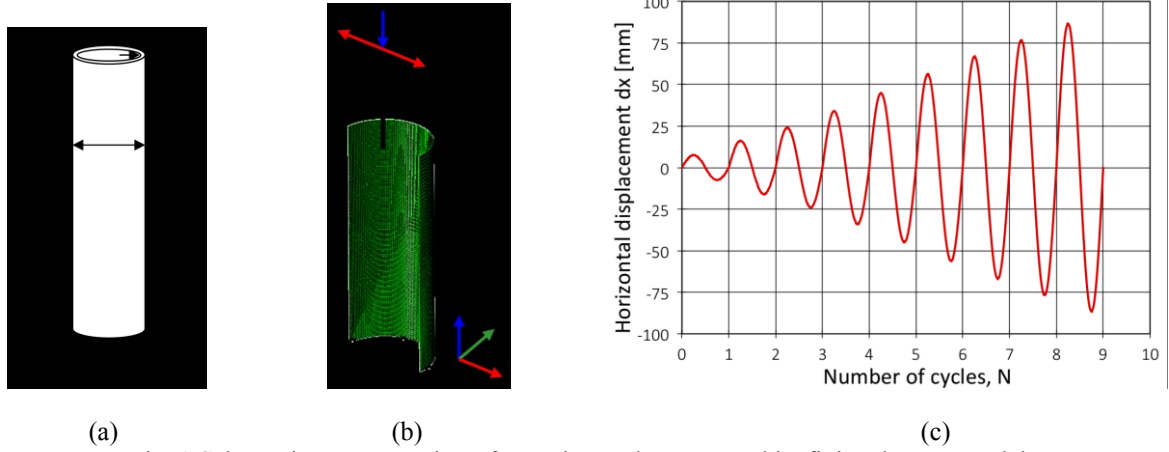

(a)   (b)   (c)

Fig. 1 Schematic representation of experimental system and its finite element model.
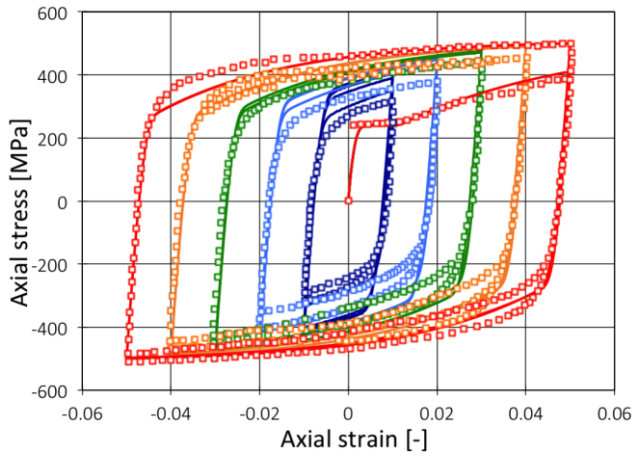

Fig. 2 Stress-strain responses of SS400 for the strain ranges =0.01, 0.02, 0.03, 0.04, 0.05 (the responses of the models with (T=0) and ($T \neq 0$) exhibit the same results under uniaxial stress cycles.)

Table 1 Material constants of SS400

Elastic moduli	$E = 210$ [GPa], $\nu = 0.3$
Initial value of yield surface	$F_0 = 294.1$ [MPa]
Isotropic hardening $F = F_0[1 + h_1\{1 - \exp(-h_2 H)\}]$	$h_1 = 0.567, h_2 = 30.0$
Stress plateau threshold	$H_p = 0.01$
Kinematic hardening $\overset{\circ}{\boldsymbol{\alpha}} = a_\alpha \left(r_\alpha F \frac{\overline{\boldsymbol{\sigma}}'}{\|\overline{\boldsymbol{\sigma}}'\|} - \sqrt{\frac{2}{3}} \boldsymbol{\alpha} \right) \|\mathbf{D}^p\|$	$a_\alpha = 34.0, r_\alpha = 0.233$
Evolution of normal yield ratio	$Re = 0.0, u = 500.0, u_s = 1.67$
Translation of similarity center	$c = 200.0, \chi = 0.9$
Tangential plasticity	$\xi = 0.9, b = 2.0$

among the principal stresses and their directions are kept constant. However, whenever a non-proportional loading condition is imposed, they tend to overestimate the material stiffness.

In order to take into account the tangential stress rate component some preliminary hypotheses [1][5] are needed:

1. the stress rate is linearly related with the tangential stretch (where A is a stress function):

$$\mathbf{D}^t = A\overset{\circ}{\boldsymbol{\sigma}}_t \tag{1}$$

2. the additive decomposition of the stretching holds:

$$\mathbf{D} = \mathbf{D}^e + \mathbf{D}^p + \mathbf{D}^t \tag{2}$$

3. the tangential stress component, and the inelastic stretch associated, are purely deviatoric[7];

4. no hardening can be generated by a stress rate component tangential to the yield surface.

The last of the assumptions (i.e. number 4), allows us to split the normal and tangential stress rate component effects, evaluating the first with the cutting-plane method and the second with a sort of 'radial return mapping'.

In order to split the aforementioned contributions, the generic stress function A is given as:

$$A = \left(\frac{T}{2G - 2GT} \right); \quad T = \xi R^b \tag{3}$$

Where T is an exponential function that depends on two material constants ξ and b, and on the similarity ratio R. Finally it is possible to write the stress rate as in Equation 4, where the tangential one is expressed in the lower expression:

$$\overset{\circ}{\boldsymbol{\sigma}} = \left\{ \mathbf{E} - \frac{\mathbf{EN} \otimes \mathbf{EN}}{M_p + tr\mathbf{NEN}} \right\} \mathbf{D} - \overset{\circ}{\boldsymbol{\sigma}}_t^* \qquad (4)$$

$$\overset{\circ}{\boldsymbol{\sigma}}_t^* = T \left(\mathbf{E} - \frac{\mathbf{EN} \otimes \mathbf{EN}}{M_p + tr\mathbf{NEN}} - \frac{1}{3}\mathbf{E} \otimes \mathbf{I} - \frac{\mathbf{EN} \otimes \mathbf{N}}{M_p + tr\mathbf{NEN}} M_p \right) \mathbf{D}$$

3. Comparison with experimental result
3.1 Description of benchmark experiment

The experimental results, compared against the numerical simulations, were conducted by Nishikawa et al[8]. Figure 1a shows the sketch of the specimen

Geometrically the sample consists of a thin wall bridge pier, with a circular cross section of 9 mm thickness, which is assumed to be made of structural steel SS400 (JIS) with a stress plateau domain right after the yielding.

### 3.2 Description of finite element model and boundary conditions

The finite element analyses were conducted by means of the commercial finite element code Abaqus/Standard ver.6.13[9]. Figure 1b displays the finite element model and boundary conditions, which reproduce the ones experimentally realized by Nishikawa[8], 1998. ,

Black thin line: Experimental result (Nishikawa, 1998)
Colored bold line: Simulation results
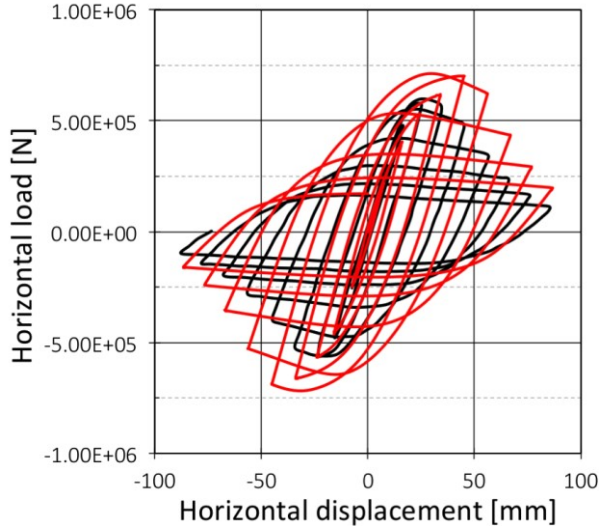
(a) w/o Tangential plasticity
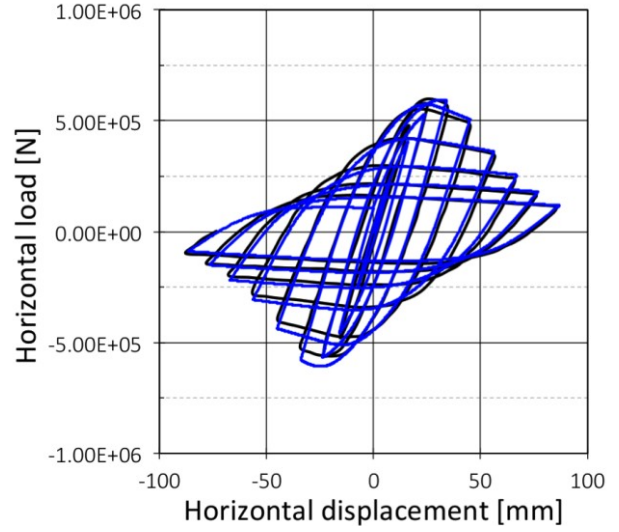
(b) w/t Tangential plasticity

Fig. 3 Relationship between horizontal displacement and horizontal load at loading point on top: (a) elastoplasticity without tangential stress rate effect and (b) elastoplasticity with tangential stress rate effect.

w/o Tangential plasticity

w/t Tangential plasticity

(a) +4d_0   (b) +5d_0   (c) +6d_0   (d) +7d_0   (e) +8d_0   (f) +9d_0
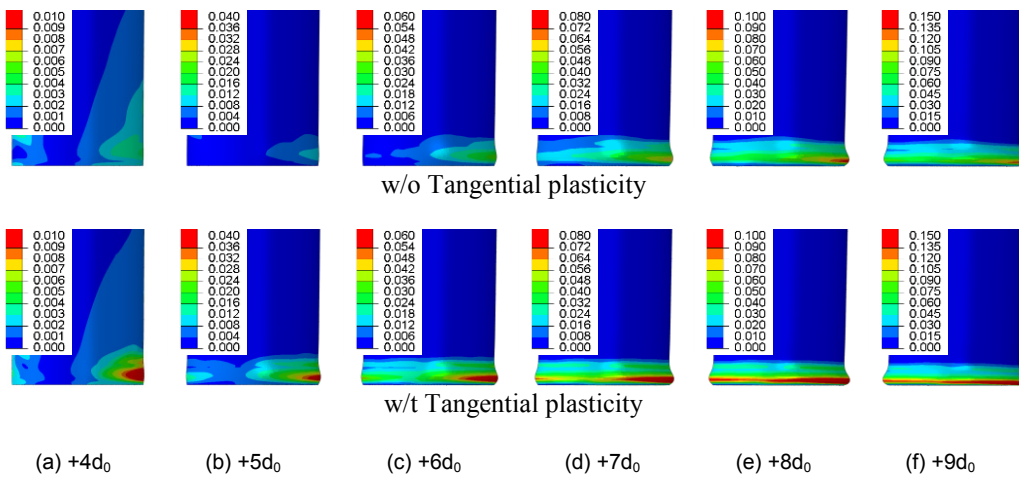
Fig. 4 Evolution of the local buckling at the bottom part of the specimen and maximum principal strain distributions: the upper figures are calculated by elastoplasticity without tangential plasticity and the lower figures are calculated by elastoplasticity with tangential plasticity.

Cyclic and Tangential Plasticity Effects for the Buckling Behavior of a Thin Wall Pier under Multiaxial and Non-proportional Loading Conditions
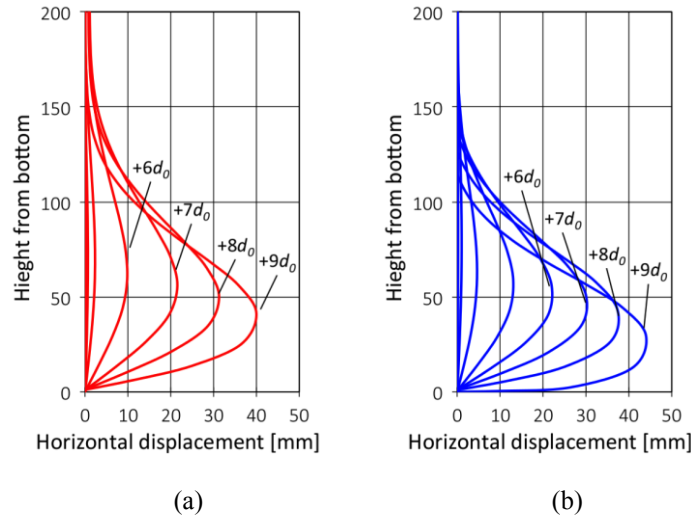

(a)   (b)

Fig. 5 Comparison of the local deformations, from +1d0 to +9d0, at the bottom of column between (a) w/o tangential plasticity and (b) w/t tangential plasticity.

(a) BS   (b) BA   (c) XU   (d) XP

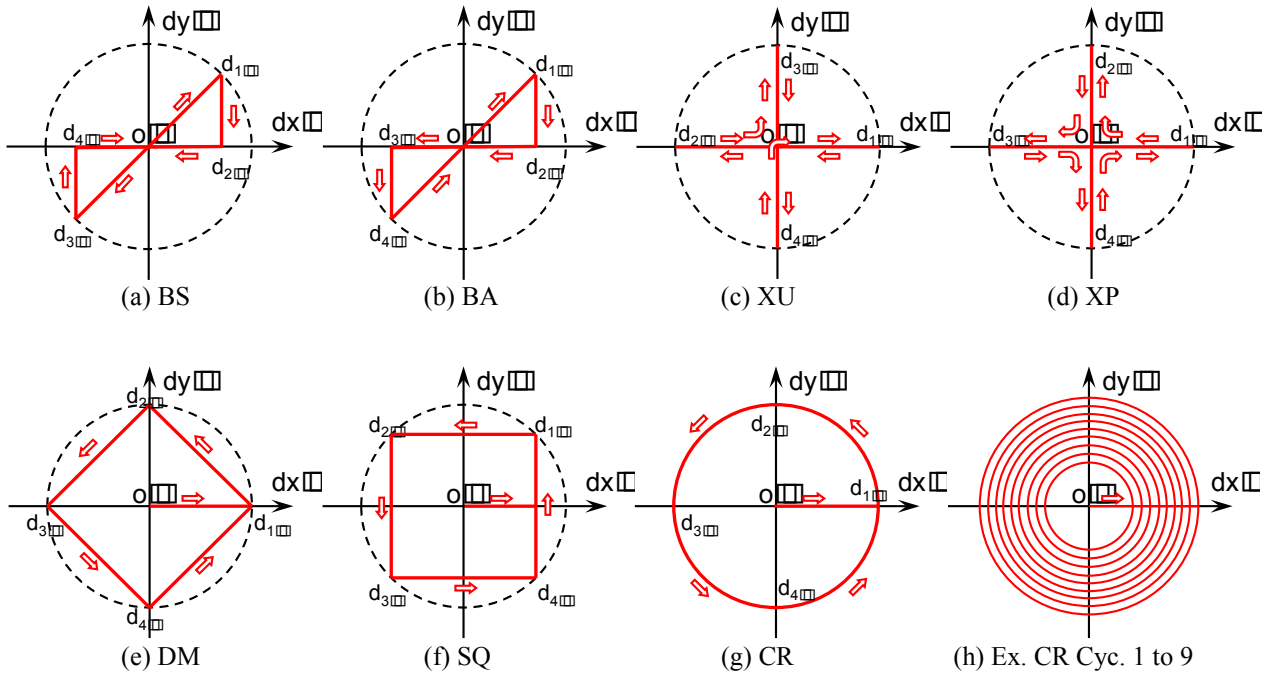(e) DM   (f) SQ   (g) CR   (h) Ex. CR Cyc. 1 to 9

Fig. 6 Schematic representation of the loading protocols.

The base of the column is fixed and the top of the column is subjected to a constant axial load and quasi-static cyclic lateral displacements shown in Fig 1b.

In order to reduce the calculation costs, the upper half of the column is modeled by beam elements (B31), the remaining part by brick elements (C3D8) and by a rigid body, which is used to connect the solid with the beam elements at the interface. Four elements have been used for the thickness discretization and the mesh density is higher in the lower part of the column, where local buckling is expected to happen.

As shown in Table1 and Fig.2, the material constants of SS400 are fitted using the experimental results performed by Nakajima[10]. On the other hand the material constants for tangential plasticity, reported in Table 1, cannot be obtained by fitting the uniaxial stress-strain curve, therefore they were defined through a trial-and-error approach, comparing the outcome of the FE simulations against the experimental results.
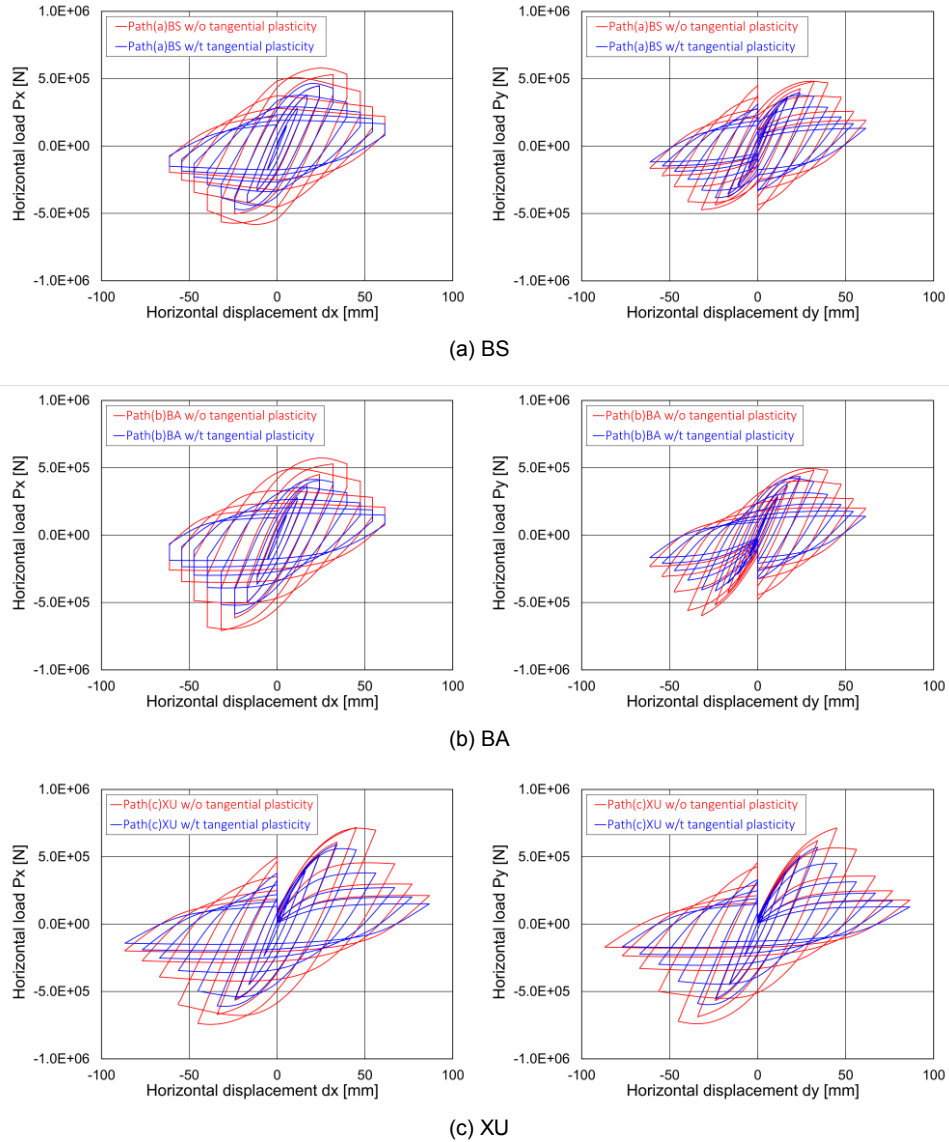
Fig. 7. Comparisons of the hysteresis loops under different loading conditions (from (a) BS to (c) XU). Left figures show the responses in the x-direction, right figures show the ones along the y-direction

3.3 Results and Discussions

The comparison between the hysteresis responses of the column obtained in the FE simulation, with ($T \neq 0$) and without tangential stress rate effect (T=0), and the experimental ones are presented in Fig.3. The curves in Fig.3b are in better agreement with the experiment than the ones obtained with the conventional plasticity (T=0). The tangential plasticity model can, in fact, capture both: the ultimate load and the decreasing of the strength for the each of the post cycle peaks during the cycles.

Figure 4 depicts the deformations carried out by using the conventional and the tangential plasticity models in the FE simulations, whereas Fig.5 compares the horizontal profiles of the sample obtained by the nodal displacements around the bottom of the column. Both of them indicate that the localization carried out by means of

the tangential plasticity algorithm tends to occur at an earlier stage, moreover it is enhanced with respect to the one resulting from the conventional plasticity model.

4. Various bi-directional loading conditions in the cross section

4.1 Loading paths

In this section seven loading paths[11] are applied to the model in order to investigate differences in response under bi-directional loading conditions. The schematic representations of these seven loading protocols are shown in Fig.6(a)~(g). Paths BS and BA trace a butterfly shape, symmetrically BS and asymmetrically BA, in the X-Y displacement space. Both XU and XP trace a cross shape path, however the number of changes of the loading direction in each cycle is different. Paths DM and SQ have

Cyclic and Tangential Plasticity Effects for the Buckling Behavior of a Thin Wall Pier under Multiaxial and Non-proportional Loading Conditions
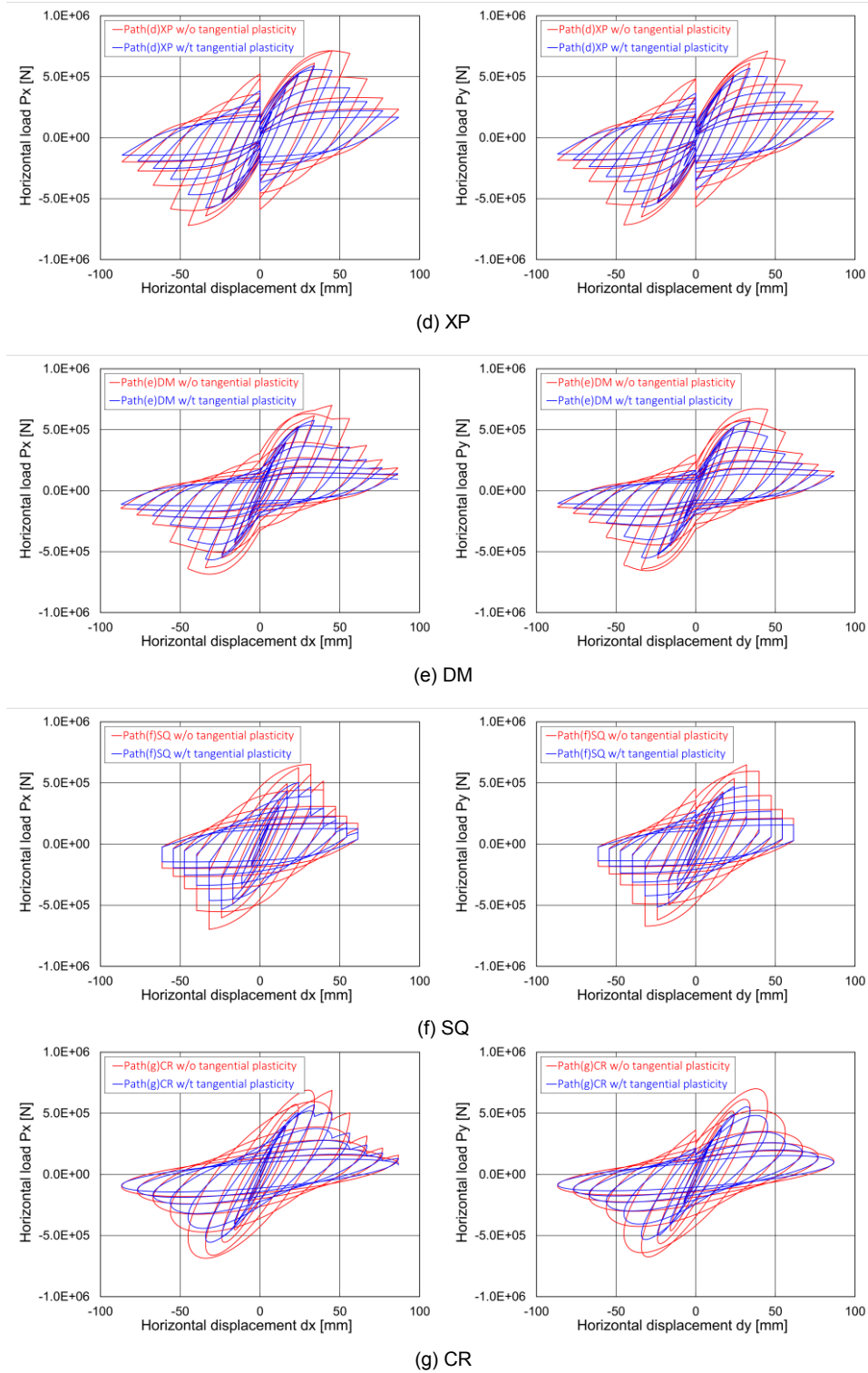

(d) XP

(e) DM

(f) SQ

(g) CR

Fig. 8 Comparisons of the hysteresis loops under different loading conditions (from (d) XU to (g) CR). Left figures show the responses in the x-direction, right figures show the ones along in the y-direction.

the same shape, but the direction at the maximum displacement in each cycle is different. Case CR traces a simple circular path. Figure 6(h) shows CR displacement history from cycle one to nine as an example. All the paths consist of nine cycles and their displacement amplitudes are increased through the cycles.

4.2 Numerical results and comparisons
Numerical calculations have been carried out using

the same material constants for both the return mapping and the tangential plasticity algorithm. Figure 7 and 8 show the hysteresis responses at the top of the specimen through the cycles. As for the case shown in Fig.3, the elastoplasticity model with tangential plasticity better estimates the minimum ultimate loads compared to the ones obtained with the conventional plasticity (T=0). In addition, the numbers of cycles necessary to reach the critical conditions are different in the two models: the results obtained by considering the tangential plasticity tend to achieve the ultimate load at an earlier stage. This means that, under operational loading conditions, the predictions simulated by the conventional elastoplasticity models may overestimate the structural resistance, with more or less serious implications for the safety factors design.

5. Concluding remarks

The paper presented the numerical results based on the extended subloading surface model incorporating the tangential plasticity effect in order to capture the material response under a non-proportional loading condition. The algorithm has been used to simulate the behavior of a thin wall bridge pier subjected to biaxial cyclic loadings.

(1) As a result of the comparison between the conventional plasticity model and the tangential plasticity model against experimental data, it can be concluded that the latter has higher predictive capability. The conventional plasticity, in fact, overestimated the ultimate load, whereas the tangential plasticity has been proved to be able to catch the experimental peak load.

(2) Decrease of the peak loads and an anticipation of the ultimate loads at earlier stage have been observed whenever the tangential relaxation has been taken into account for all of the seven bi-directional loading paths.

This indicates the importance of considering the tangential plasticity effect in order to achieve more accurate and reliable predictions under operational loading conditions. The further validation of material constants for tangential plasticity is left as a future work.

References

[1] Hashiguchi, K., and Tsutsumi, S., "Elastoplastic constitutive equation with tangential stress rate effect," Int. J. Plasticity, vol. 17, page 117-145, 2001.

[2] Hashiguchi, K., Pfeiffer, F., Wriggers, P., "Elastoplasticity theory," Lecture notes in applied and computational mechanics, Springer, Berlin, 2009.

[3] Hashiguchi, K., and Mase, T., "Subloading surface Model and its Return-mapping Formulation," ACTA 60th Nat. Congr. Of Theoretical & Applied Mechanics, Japan, 2011.

[4] Hashiguchi, K., Suzuki, N., and Ueno, M., "Elastoplastic deformation analysis by return-mapping and consistent tangent modulus tensor based on subloading surface model (1st report, formulation of return-mapping)," Transaction of the JSME, vol. 80, No. 812, 2014. (in Japanese)

[5] Tsutsumi, S., and Hashiguchi, K., "General non-proportional loading behavior of soils," Int. J. Plasticity, vol. 21, page, 1941-1969, 2005.

[6] Simo, J. C., and Oritz, M., "A unified approach to finite deformation elastoplasticity based on the use of hyperelastic constitutive equations," Compt. Meth. Appl. Mech. Eng., vol. 49, page 221-245, 1985.

[7] Rudnicki, J. W., and Rice, J. R., "Conditions for localization in pressure-sensitive dilatant materials," J. Mech. Phys. Solids, vol. 23, 371-394, 1975.

[8] Nishikawa, K., Yamamoto, S., Natori, T., Terao, K., Yasunami, H., and Terada, M., "Retrofitting for seismic upgrading of steel bridge columns," Eng. Struct., vol. 20, page 540-551, 1998.

[9] Abaqus Users Manual, Version 6.13-1, Dassault Systémes Simulia Corp., Providence, RI.

[10] Nakajima, N., and Yamada, M., "Hysteresis Loop Characteristics of Structural Carbon Steel SS400 in Very Large Plastic Zones," J. Struct. Constr. Eng. AIJ, No. 536, page 17-22, 2000. (in Japanese)

[11] Ucak, A., Tsopelas, P., "Load Path Effects in Circular Steel Columns under Bidirectional Lateral Cyclic Loading", J. Struct. Eng, ISSN (online): 1943-541X, 2014